Supporting Information

High Efficiency Thin Upgraded Metallurgical-Grade Silicon Solar Cells on Flexible Substrates

Jae Young Kwon[1]*, Duck Hyun Lee[1]*, Michelle Price[2], Stephen Maldonado[2], Anish Tuteja[1#], Akram Boukai[1#]

[1]*Department of Materials Science and Engineering, University of Michigan, Ann Arbor, MI, United States*

[2] *Department of Chemistry, University of Michigan, Ann Arbor, MI, United States*

[#]Contact E-mail: boukai@umich.edu, atuteja@umich.edu

EXPERIMENTAL

Upgraded metallurgical-grade (UMG) Si solar microcells

A p-type UMG-Si wafer was polished in chemical mechanical polisher (CMP IPEC 472). Then, a 3 μm thick layer of photoresist (SPR 220-3.0, Shipley) was spin-coated on the wafer and baked for 90 sec at 115 °C. The lateral dimensions (9 μm × 650 μm) and layout of the microcells were defined by 365 nm UV exposure (Karl Suss MA6 mask aligner) and developing in AZ300 MIF. Inductively coupled plasma reactive-ion etching (ICP-RIE, STS Pegasus) formed ~25 μm deep trenches (Fig. S2a) in the exposed regions, and the photoresist was stripped (Baker PRS 2000). For the selective area doping of the microcells, 500 nm of SiO_2 was deposited with plasma-enhanced chemical vapor deposition (PECVD) at 200 °C, and patterned by photolithography, BHF etching and photoresist stripping. Solid-state targets of boron (BN-1250, Saint Gobain) and phosphorous (PH-1000N, Saint Gobain) were used as doping sources and were diffused into the wafer at 1000 °C under Ar ambient for 15 min (boron) and 20 min (phosphorous) in a tube furnace. The remaining dopant was cleaned in diluted HF solution (HF:H_2O = 1:1) for 1 min. SiO_2(100 nm)/Si_3N_4(300 nm) were deposited with PECVD system at 200 °C, and thin Ni film (50 nm) was deposited with angled deposition with E-beam evaporation. The UMG-Si wafer was diced (ADT 7100 Dicing saw), and etched with XeF_2 etching (Xactix, 3 mT, 40 sec per cycle, 8 cycles). This process provided freestanding microcell arrays (Fig. 1b and c) with a thickness of 17 μm. The Ni layer was removed in an etching solution (HCl/H_2O_2/H_2O = 1:1:5). The microcell arrays were doped with boron by spin coating spin-on-dopant (Filmtronics) followed by

annealing at 1000 °C for 3 min to create backside doping of the microcells. Finally oxide/nitride layers were removed in HF solution (HF/H_2O = 1:1).

Transfer Printing and Finishing the Solar Cells

Elastomeric printing stamps were prepared by mixing PDMS prepolymer and cross-linking agent (Sylgard 184, Dow Corning Corp.) at a volume ratio of 10:1 and curing at 80 °C for 2 hrs. The stamps were placed against the donor pieces and were applied with sufficient stress. Then, they were peeled off quickly to release the microcells from the donor substrate, and ink them onto the surface of the stamp. Receiving substrates were prepared by cleaning a glass slide with UV/O_3 for 10 min and spin coating with a photo-curable polymer (NOA61, Norland Products Inc.). The PDMS stamp inked with microcells was placed against this substrate and the whole system was cured in UV light for ~15 min. Then the PDMS stamp was peeled off leaving the microcells embedded in a NOA matrix (Fig. 1d). Interconnects on the microcells-inked NOA61 substrate, were made by Cr/Au (30 nm/400 nm) sputtering followed by spin coating photoresist (AZ 5214, Shipley) for photolithography. The exposed metal layers were removed in Au etchant Type TFA and CR-14 Cr etchant to define the electrodes. The remaining photoresist was stripped in acetone to finish the device (Fig. 1e).

Silver nanoparticles and Si nanopillar arrays formation

The surface of UMG-Si was neutrally treated by a random copolymer brush. A thin film (100 nm) of asymmetric block copolymers, polystyrene-block-poly(methyl methacylate)s (PS-b-

3

PMMAs) forming cylindrical nanostructures (molecular weight: PS/PMMA-140k/60k, PMMA cylinder diameter: 34 nm, center to center distance between neighboring cylinders: 64 nm & molecular weight: PS/PMMA-46k/21k, PMMA cylinder diameter: 18 nm, center to center distance between neighboring cylinders: 34 nm) were spin-coated onto the wafer surface. After high temperature annealing at 190 °C, the substrates were irradiated with UV and subsequently rinsed with acetic acid and water to remove PMMA cylinder cores and crosslink the PS matrix. The substrate was further treated in oxygen plasma for 15 sec in order to remove the remnant cylinder cores (Fig. 2b). The Ag thin film (30 nm) was deposited over the PS template. After the deposition process, the remaining PS nanoporous template was lifted-off by sonicating in toluene. Through this procedure, Ag nanoparticles having uniform size and arrayed following the hexagonal lattice of the nanotemplates were formed on the Si surface (Fig. 2c). Using the remaining Ag nanoparticles as an etching mask, the Si substrate was etched by RIE to produce dense Si nanopillar arrays (Fig. 2d).

Quantum efficiency measurement

Quantum efficiency measurements were obtained with an Oriel 150 W Xe arc lamp (Newport) and a quarter-turn single-grating monochromator (Newport). Sample measurements were recorded with chopped illumination (15 Hz), and a quartz beam splitter was used to simultaneously record the light output intensity with a separate Si photodiode (Newport) to adjust for fluctuations in lamp intensity. The wavelength-dependent external quantum yield values were measured at short-circuit for each device, and the absolute photocurrents were measured by a digital PAR 273 potentiostat. The output current signal was connected to a Stanford Instruments

SR830 lock-in amplifier, and the output signals from the lock-in amplifier and the reference Si photo-diode were fed into a computer controlled by custom-written LabVIEW software.

Plasmonic effect simulation

The FDTD software (Lumerical Solutions, Inc.) was used for the simulation of the electric field intensity enhancement and the power absorption per unit volume on the surface of Ag nanoparticle and Si nanopillar arrays on Si. The material properties of Ag was taken from the material database of Johnson and Christy,[1] and that of Si was taken from the material database of Palik.[2] The dimensions and the layout of the structures were set to be the same with the real device. The dimensions of the rectangular Si substrate was set to be 300 nm by 300 nm with a thickness of 10 μm. The incident light is propagating along the z-axis and is polarized along the *x*-axis. The light source was placed in the center of the structures, 100 nm above the silicon substrate, with a wavelength ranging from 400 nm to 1100 nm. The electric field and reflective index were calculated in the given structures. The power absorption per unit volume was calculated from the divergence of the Poynting vector with following equation:

$$P_{abs} = -0.5 real(\vec{\nabla} \cdot \vec{P})$$

SUPPORTING FIGURES

Figure Legends

Figure S1. A schematic illustration of the steps for the preparation of ultrathin UMG-Si solar microcells and the process of integrating them in to the completed modules.

Figure S2. a, Top SEM image of prepared trenches for MG-Si solar microcells. **b** and **c**, Cross sectional SEM images of microcell arrays after 4 cycles (**b**) and 8 cycles (**c**) of XeF_2 dry etching. A thin metal film (Ni, 50 nm) deposited with angled evaporation was used for the etching mask. **d**, *J–V* curves for 180 μm thick bulk UMG-Si cell and microcell module. **e**, *J–V* curves of as-prepared microcell module and 3 month old microcell module. The prepared microcell module had good sustainability over a period of 3 months. **f**, Optical image of a microcell module with Ag nanoparticle/Si nanowire array structure. Both block copolymer lithography and reactive ion etching were not affected by the flexibility and transparency of the microcell module.

Figure S3. Calculated absorbance spectrums for 180 μm thick Si and 17 μm thick Si. The absorbance of 17 μm thick Si decreased significantly in the long wavelength region. This calculation was executed using the Essential Macleod software (ver. 9.4).[3]

Figure S4. Diffuse reflectance (**a**) and specular reflectance (**b**) curves for the as-doped UMG-Si (black), Ag nanoparticle (*D*: 18 nm, *t*: 30 nm) on UMG-Si (magenta), Ag nanoparticle/Si nanopillar arrays prepared with 18 nm Ag nanopillars on UMG-Si (blue), Ag nanopillars (*D*: 34 nm, *t*: 30 nm) on UMG-Si (green) and Ag nanoparticle/Si nanopillar arrays prepared with 34 nm Ag nanoparticles on UMG-Si (red). **c**, The absorbance difference between the 18 nm Ag nanoparticles and the 34 nm Ag nanoparticles on top of the doped UMG-Si samples. As the size of Ag nanoparticles increased, a "blue-shift" was observed.

Figure S5. Energy dispersive spectroscopy (EDS) curves (**a**) and *J–V* curves (**b**) for a UMG-Si cell both before (blue) and after (red) Ag nanoparticle removal. **c**, Efficiency enhancement of UMG-Si cells caused by Ag nanoparticles and Ag nanoparticle/Si nanowire array.

Figure S6. The simulated structures for Ag nanoparticles (**a**, **b** and **c**) and Ag nanoparticles/Si nanopillars (**d**, **e** and **f**) on a Si substrate. The perspective views (**a** and **d**), x-y plane views (**b** and **e**) and x-z plane views (**c** and **f**) are also shown. The diameter and height of the Ag nanoparticles (**a**, **b** and **c**) on top of Si were 34 nm and 30 nm, while the diameter and height for the Ag nanoparticles in the Ag nanoparticle/Si nanowire arrays (**d**, **e** and **f**) were 23 nm and 18 nm. The height of Si nanowire array was 120 nm.

Figure S7. The simulated power absorption per unit volume of bare (**a**), Ag nanoparticle (**b**) and Ag nanoparticle/Si nanopillar array (**c**) on Si under an incident light of 700 nm for x-z plane. The dotted lines show the outline of simulated structures. The power absorption calculations show the absorption enhancement effect at the Si substrate in the presence of Ag nanoparticle and Ag nanoparticle/Si nanowire array structures.
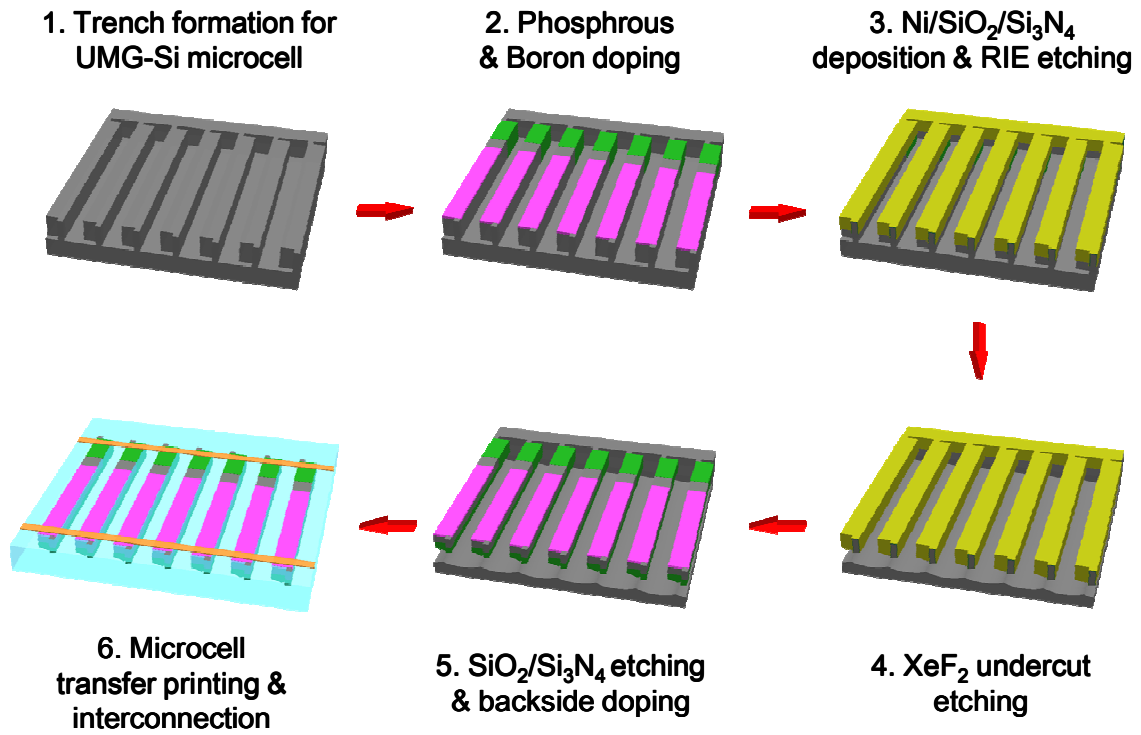
Figure S1

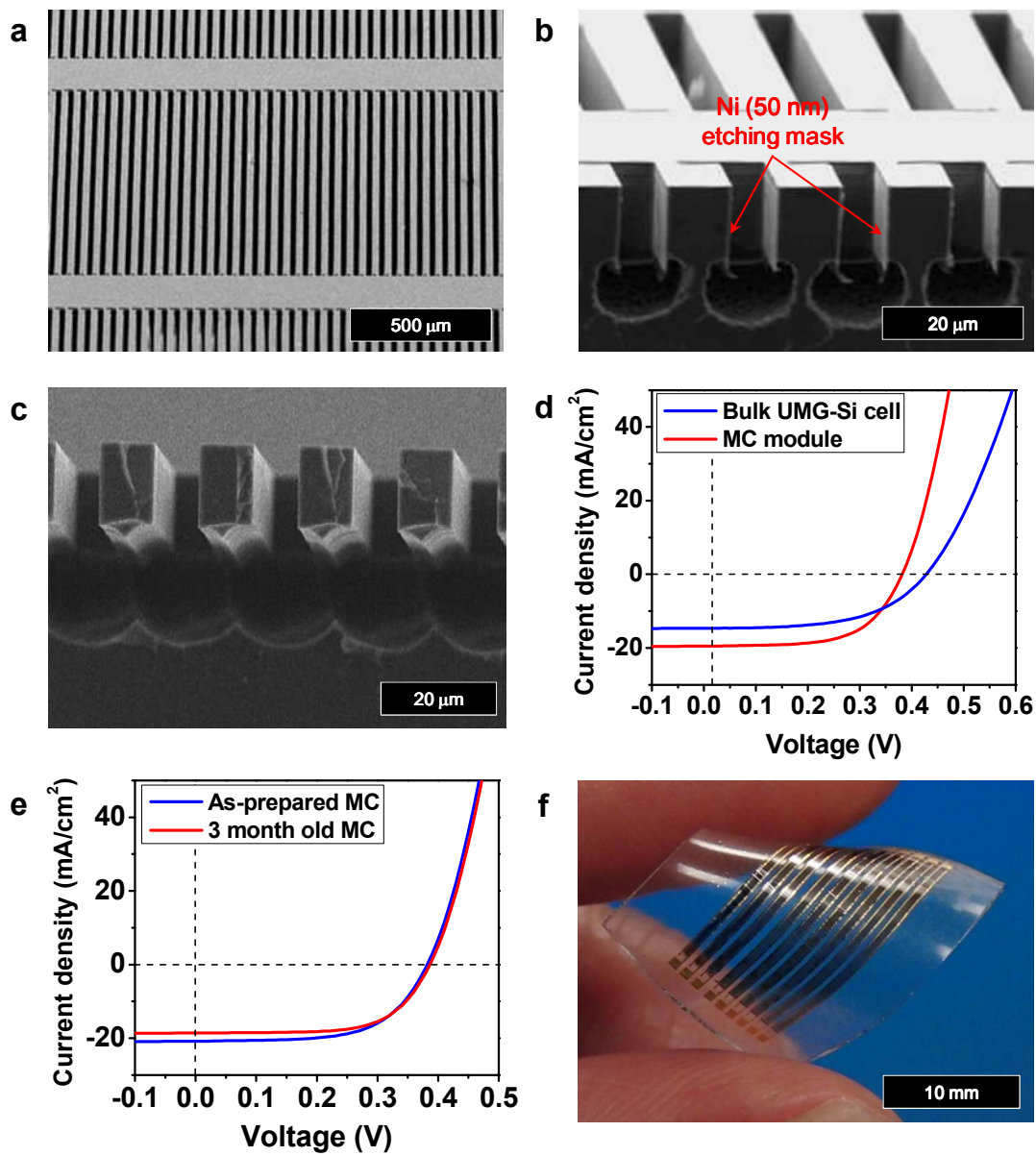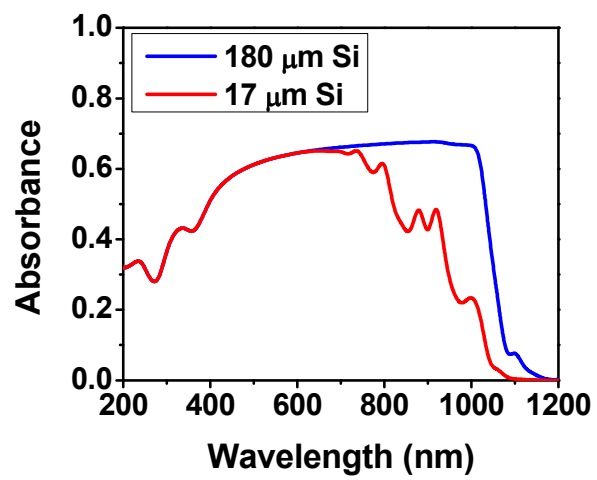1. Trench formation for
UMG-Si microcell

2. Phosphrous
& Boron doping

3. Ni/SiO_2/Si_3N_4
deposition & RIE etching

6. Microcell
transfer printing &
interconnection

5. SiO_2/Si_3N_4 etching
& backside doping

4. XeF_2 undercut
etching

Figure S2

Figure S3

Figure S4

a

Diffusion Reflectance vs Wavelength (nm)

Legend:
- Doped UMG-Si
- AgNP, 18 nm
- AgNP/SiNA, 18 nm
- AgNP, 34 nm
- AgNP/SiNA, 34 nm

b

Specular reflectance vs Wavelength (nm)

Legend:
- Doped UMG-Si
- AgNP, 18 nm
- AgNP/SiNP, 18 nm
- AgNP, 34 nm
- AgNP/SiNP, 34 nm

c

Δ Absorbance vs Wavelength (nm)

Legend:
- AgNP, 18 nm
- AgNP, 34 nm

Blue - shift

11

Figure S5

Figure S6

a

b
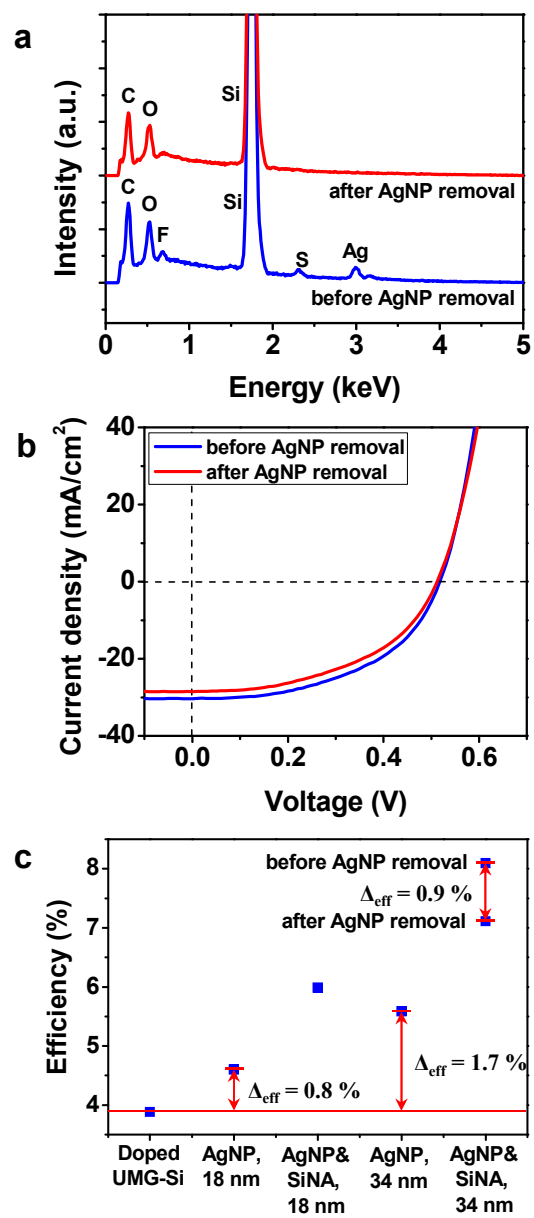
34 nm
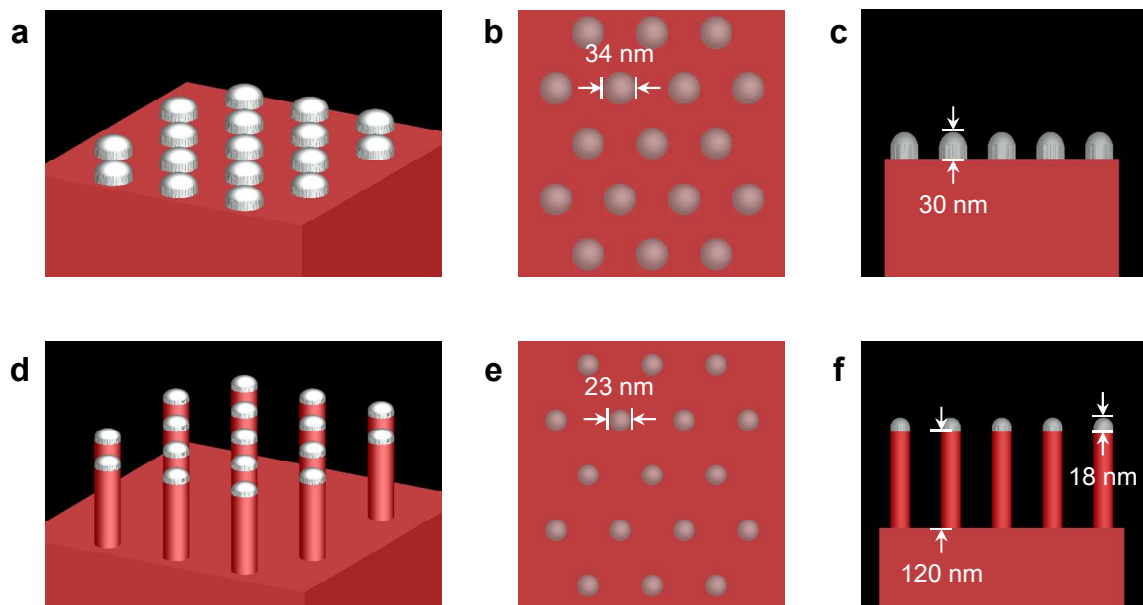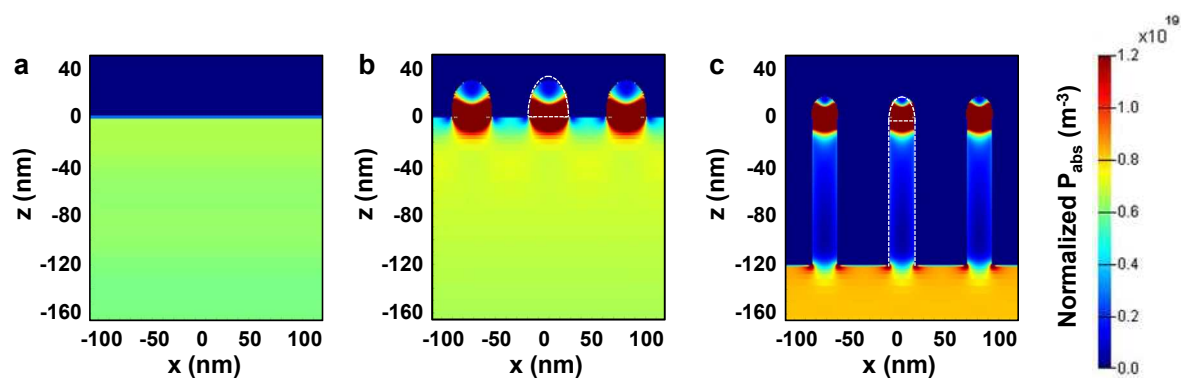
c

30 nm

d

e

23 nm

f

18 nm

120 nm
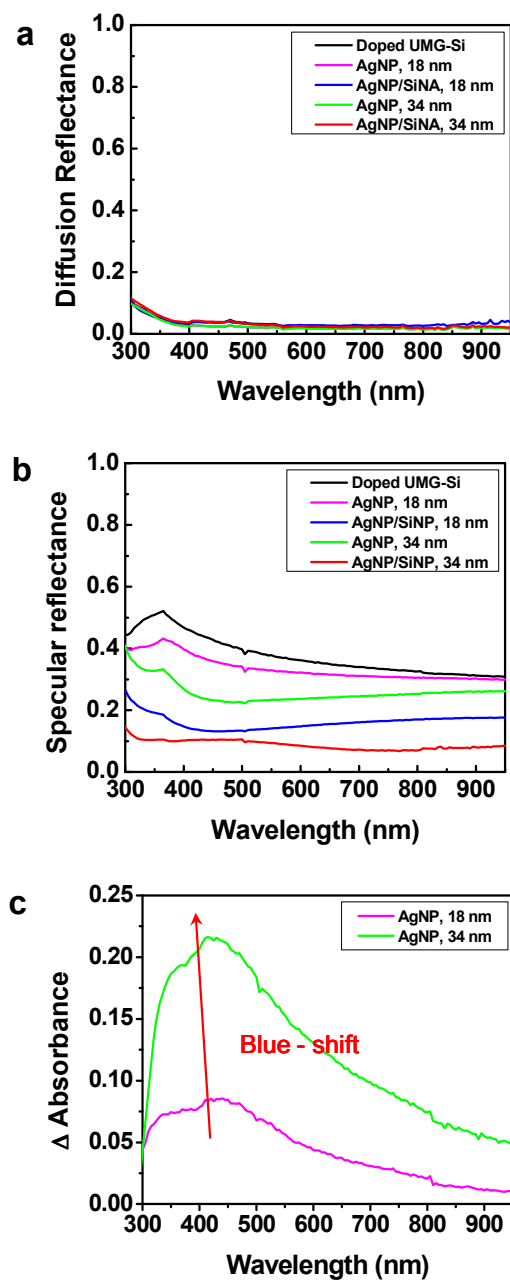
Figure S7

SUPPORTING TABLES

Table S1. J-V characteristics of the 180 μm thick bulk UMG-Si cell and the prepared microcell module (Fig. S2d).

Microcells	J_{SC} (mA/cm^2)	V_{OC}(V)	FF	η (%)
Doped UMG-Si	14.63	0.47	0.55	3.77
Ribbon Microcell	19.55	0.40	0.60	4.69

Table S2. J-V characteristics of as-prepared microcell module and 3 month old microcell module (Fig. S2e).

Microcells	J_{SC} (mA/cm^2)	V_{OC}(V)	FF	η (%)
As-prepared microcell module	19.55	0.40	0.60	4.69
3 month old microcell module	19.47	0.39	0.60	4.56

Table S3. J-V characteristics of before and after Ag nanoparticle etching (Fig. S5b).

Cells	J_{SC} (mA/cm^2)	V_{OC}(V)	FF	η (%)
Before Ag nanoparticle etching	29.98	0.49	0.55	8.08
After Ag nanoparticle etching	27.70	0.48	0.54	7.18

1.   Johnson, P. B.; Christy, R. W. *Phys Rev B* **1972,** 6, 4370-4379.
2.   Palik, E. D., *Handbook of Optical Constants of Solids*. Academic Press: 1991.
3.   Chen, T., Numerical Simulations of Temperature-dependence on Distributed Bragg Reflector (DBR) and Performance Analyses for Proton-Implant/Oxide Confined VCSEL:

Comparison with Transmission Matrix, Matrix Calculating Methods and Macleod Model. In *Laser Pulse Phenomena and Applications*, Duarte, F. J., Ed. InTech: 2010.